PHYSICAL REVIEW D **92,** 033009 (2015)

Constraints on dark photon from neutrino-electron scattering experiments

S. Bilmiş,[1] I. Turan,[1,*] T. M. Aliev,[1] M. Deniz,[2,3] L. Singh,[2,4] and H. T. Wong[2]
[1]*Department of Physics, Middle East Technical University, Ankara 06800, Turkey*
[2]*Institute of Physics, Academia Sinica, Taipei 11529, Taiwan*
[3]*Department of Physics, Dokuz Eylül University, İzmir 35160, Turkey*
[4]*Department of Physics, Banaras Hindu University, Varanasi 221005, India*
(Received 2 April 2015; published 21 August 2015)

A possible manifestation of an additional light gauge boson A', named a dark photon, associated with a group $U(1)_{B-L}$, is studied in neutrino-electron scattering experiments. The exclusion plot on the coupling constant g_{B-L} and the dark photon mass $M_{A'}$ is obtained. It is shown that the contributions of interference terms between the dark photon and the Standard Model are important. The interference effects are studied and compared with data sets from TEXONO, GEMMA, BOREXINO, and LSND, as well as CHARM II experiments. Our results provide more stringent bounds to some regions of parameter space.

DOI: 10.1103/PhysRevD.92.033009 PACS numbers: 13.15.+g, 12.60.-i, 14.70.Pw

I. INTRODUCTION

The recent discovery of the long-sought Standard Model (SM) Higgs at the Large Hadron Collider is the last missing piece of the SM, which has strengthened its success even further. Of course, this does not change the fact that there are the issues of neutrino mass, the presence of dark matter, etc., and thus the SM is an effective theory whose range of validity has to be tested in either direction from the weak scale. While the scale of new physics sets up one boundary at the higher end, the mass scale of the neutrinos could be considered one of the fundamental scales in physics at the lower tail, around which the SM's validity should also be questioned. For instance, neutrino nucleus coherent scattering has not been observed yet [1], which will test the SM at very low energies.

In the quest for new physics, the limitations of the SM can be tested through high-energy frontiers, as well as through the intensity frontier with high-precision experiments, which are considered to be complementary to the direct searches at high energies. There are numerous experimental results, such as the anomalous magnetic moment of the muon [2,3], the smallness of the electric dipole moment of the neutron [2,4], the electric charge radius puzzle of the proton [5], the positron excess in cosmic rays without antiproton abundance (first seen by an ATIC experiment [6] and later confirmed by PAMELA [7] and FERMI [8] satellite experiments), as well as an INTEGRAL satellite experiment observation of a very bright 511 keV line [9] together with other puzzling results coming out of the DAMA/LIBRA [10] and EGRET [11] collaborations and also the recent AMS-02 experiment announcement about the positron excess even with a sharper rise up to 300 GeV energies [12], none of which can be explained within the SM. Hence, new physics scenarios beyond the SM are needed. Even though finding a way out to one or two of these is a step, the real ambitious challenge is to find a framework where all or at least most of all of these puzzling inconsistencies find themselves a remedy without violating any of the existing data.

As a remedy to some of these issues, we will consider a hidden sector scenario where the existence of a dark photon may alter significantly the neutrino-electron scattering data, or at least its gauge coupling and mass could be constrained with the use of the data. There are various neutrino-electron scattering experiments, which are mainly TEXONO [13–15], BOREXINO [16], and GEMMA [17], as well as LSND [18] and CHARM II [19]. A light dark photon could be searched using these data.

The paper is organized as follows: In Sec. II, the idea of the hidden sector and some details of the considered model will be described. In Sec. III, the details of neutrino-electron scattering in the SM as well as the $U(1)_{B-L}$ dark photon scenario will be given. Pure dark photons as well as interference contributions to the differential cross sections of various neutrino-electron scattering processes are presented. In Sec. IV, our results are compared with the existing results in literature. Especially, the interference effects are discussed in detail, and its importance for some cases is stressed. Section V contains our conclusions.

II. HIDDEN SECTOR AS A BEYOND-THE-STANDARD-MODEL SCENARIO

The idea of the existence of a so-called hidden sector interacting with the SM through various portals (more on portals is below) is one such extension of the SM aiming to explain some of the above issues. With a single particle from the hidden sector being singlet under the SM gauge group, there is no way to couple with the visible part other than its gravitational effects, which will be suppressed by the Planck scale, putting them out of reach of any current experimental search (it should then truly be called the

*ituran@metu.edu.tr

hidden sector). So for testable scenarios, more than one hidden sector field should play a role in the portal.

One may consider couplings of the form $\mathcal{L} = \sum_{l,m} \mathcal{O}_{\rm HS}^{(l)} \mathcal{O}_{\rm SM}^{(m)}$, where $\mathcal{O}_{\rm HS}(\mathcal{O}_{\rm SM})$ are some hidden (SM) sector operator, and if the sum of the dimensions of the operators is $l + m = 4$, there will be no suppression due to high cutoff scale. Such SM operators at the lowest order are known as portals, like the vector portal, Higgs portal, neutrino portal, axion portal, etc.

Among many possible portals mentioned above, the so-called vector portal assumes a hidden sector vector boson coupled to the SM gauge boson(s) through a kinetic mixing which could be generated through one loop by exchange of a heavy messenger having nonzero charge under both the SM and hidden sector gauge groups. There are alternatives one can consider for the gauge group from the hidden sector, but the simplest choice would be an Abelian symmetry as an extra $U(1)$, dubbed as $U(1)'$, which is well motivated from both the top-down (grand unification, string theory, etc.) and the bottom-up (dark matter and other issues mentioned above) approaches in extending the SM to tackle the puzzles at hand.

With a $U(1)'$ hidden sector gauge symmetry, it mixes with the corresponding SM $U(1)_Y$ in the same representation through a renormalizable operator by a kinetic-term mixing mechanism (this is a way to avoid otherwise strong theoretical and experimental constraints due to this new interaction). The hidden sector gauge field of $U(1)'$ is called a hidden or dark photon. The mixing parameter ϵ is constrained by the scale of the messenger fields. Further suppression occurs when the SM gauge group is embedded into a bigger grand unified picture in the top-down approach where the leading contributions would be two loop. In the bottom-up approach, breaking the $U(1)'$ symmetry at very light scales is not very unusual, since it seems that neutrino mass differences indicate the existence of another fundamental scale in that regime. If this gauge boson plays the role of dark matter for explaining astrophysical anomalies like positron excess [6–8], the 511 keV line [9], and the 3.55 keV photon line [20], etc., this gauge boson should have mass below the electroweak scale.

Even though the idea of very light vector bosons from the hidden sector in the form of a dark photon is not new [21,22], their effects on various SM processes at low energies in intensity frontiers have recently received great attention, which might be partly due to lack of any new physics signal at the Large Hadron Collider.

The allowed interactions of the dark photon with the SM particles depend on the theoretical framework. There are two main approaches to the way to couple the dark photon sector with the SM. One common practice is to make the dark photon mix with the photon through a kinetic mixing so that, like the SM photon, its coupling only with the charged fermions would be induced. The mass of the dark photon and a kinetic mixing parameter are the only additional ingredients of the model. Note that even though the new gauge coupling constant is involved in the definition of the kinetic mixing parameter ϵ through a one-loop diagram, it does not affect directly the dark photon coupling to the SM particles.

Another way to connect the dark photon sector with the SM is through a $U(1)$ gauging, like $U(1)_{\rm B-L}$, where the dark photon as the gauge field of the group interacts with any SM particle with a nonzero B − L number at tree level. Here the new gauge coupling constant and the dark photon mass serve as the free parameters by ignoring the kinetic mixing. Even though the consideration of these on a one-at-a-time basis is mostly adopted in order to have better predictability power, there is no prior reason not to allow both at the same time. Our aim is to bound the coupling constant $g_{\rm B-L}$ directly rather than translating the bound on ϵ.

Let us consider the Lagrangian including both the kinetic mixing with the hypercharge $U(1)_Y$ and the B − L coupling. We have

$$\mathcal{L} = -\frac{1}{4} B'^2_{\mu\nu} - \frac{1}{4} F''^2_{\mu\nu} + \frac{1}{2} \epsilon' B'_{\mu\nu} F''^{\mu\nu} + \frac{1}{2} M^2_{A''} A''^2_\mu + g_Y j^\mu_B B'_\mu + g_{B-L} j^\mu_{B-L} A''_\mu + \cdots, \tag{1}$$

where B'_μ and A''_μ are the gauge fields of the $U(1)_Y$ and $U(1)_{\rm B-L}$ groups, respectively, and the currents are defined as

$$j^\mu_B = \frac{e}{g_Y} (\cos\theta_W j^\mu_{\rm em} - \sin\theta_W j^\mu_Z),$$
$$j^\mu_{B-L} = (B-L) \bar{f} \gamma^\mu f = -\bar{\ell} \gamma^\mu \ell - \bar{\nu}_\ell \gamma^\mu \nu_\ell + \frac{1}{3} \bar{q} \gamma^\mu q.$$

The kinetic mixing can be eliminated by rotating the fields from (B'_μ, A''_μ) to (B_μ, A'_μ) as given in first order in ϵ', $B''_\mu \simeq B_\mu + \epsilon' A'_\mu$, $A''_\mu \simeq A'_\mu$, and we get

$$\mathcal{L} = -\frac{1}{4} B^2_{\mu\nu} - \frac{1}{4} F'^2_{\mu\nu} + \frac{1}{2} M^2_{A'} A'^2_\mu + g_Y j^\mu_B B_\mu + g_{B-L} j^\mu_{B-L} A'_\mu + e\epsilon j^\mu_{\rm em} A'_\mu + \cdots, \tag{2}$$

where $M_{A''} \simeq M_{A'}$ and $\epsilon \equiv \epsilon' \cos\theta_W$. The original kinetic mixing term in Eq. (1) turns into the last term in Eq. (2), which represents the interaction of the dark photon with the charged matter field with coupling $e\epsilon$. Since without the B − L gauging the dark photon does not couple with the neutrinos at tree level, we prefer to consider B − L and set the kinetic mixing to zero. We will focus on the search for dark photons with neutrino experiments, which have the advantage of being a purely leptonic process.

The formulation of this work and the corresponding analysis are based on Dirac neutrinos. However, the differences between Dirac and Majorana neutrinos within

the SM framework in neutrino-electron scatterings are expected to be small [23,24] at the level of $(\frac{m_\nu}{E_\nu})^2 < 10^{-14}$ for typical values of $m_\nu < 0.1$ eV and $E_\nu >$ MeV for the experimental configurations adopted in this work.

III. NEUTRINO-ELECTRON SCATTERING

A. Standard Model expressions

Neutrino interactions are purely leptonic processes with robust SM predictions. Hence, searching physics beyond the SM in neutrino-electron scattering turns out to be a good alternative to collider searches. In the SM, the $\nu_e - e$ scattering takes place via both charged and neutral currents. However, the $\nu_\alpha e^-$ scattering in which α corresponds to μ or τ occurs only due to neutral current. See Fig. 1 for the relevant diagrams.

The differential cross section in the lab frame of the electron in the SM can be written as

$$\left[\frac{d\sigma}{dT}(\nu e^- \to \nu e^-)\right]_{\rm SM} = \frac{2G_F^2 m_e}{\pi E_\nu^2}(a^2 E_\nu^2 + b^2(E_\nu - T)^2 - ab m_e T), \quad (3)$$

where G_F is the Fermi coupling constant, T is the recoil energy of the electron, E_ν is the energy of the incoming neutrino, and m_e is the mass of the electron. The differential cross sections differ depending on the neutrino flavor, i.e. depending on parameters a and b. The values of a and b are given in Table I.

The maximum recoil energy of the electron depends on the mass of the electron as well as incoming neutrino energy:

$$T_{\rm max} = \frac{2E_\nu^2}{m_e + 2E_\nu},$$

which also means that the minimum neutrino energy required to give the electron a recoil energy T is

$$E_{\nu_{\rm min}} = \frac{1}{2}\left(T + \sqrt{T^2 + 2Tm_e}\right). \quad (4)$$

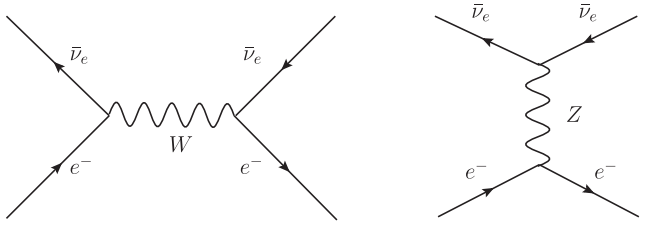

FIG. 1. Electron neutrino-electron scattering interaction takes place via both charged and neutral currents. For neutrinos other than the electron type, only the neutral current is involved.

TABLE I. The parameters a and b in the SM cross section expression in Eq. (3).

Process	a	b
$\nu_e e^- \to \nu_e e^-$	$\sin^2\theta_W + \frac{1}{2}$	$\sin^2\theta_W$
$\bar{\nu}_e e^- \to \bar{\nu}_e e^-$	$\sin^2\theta_W$	$\sin^2\theta_W + \frac{1}{2}$
$\nu_\alpha e^- \to \nu_\alpha e^-$	$\sin^2\theta_W - \frac{1}{2}$	$\sin^2\theta_W$
$\bar{\nu}_\alpha e^- \to \bar{\nu}_\alpha e^-$	$\sin^2\theta_W$	$\sin^2\theta_W - \frac{1}{2}$

Any deviation of the recoil energy spectra of electrons from what the SM predicts could be taken as a smoking gun for new physics. Our earlier works include studies of nonstandard interaction parameters as well as unparticle and noncommutative physics [25,26]. The dark photon contributions as well as its interference effects with the SM are explored in the next section.

B. Very light vector boson contributions

Now, let us calculate the contributions of the new light vector boson to the neutrino-electron scattering processes. But first, a few comments are in order. The general form of the renormalizable Lagrangian is given in Eq. (2), where the dark and conventional photons can be mixed via a kinetic term as mentioned earlier. Analyses of the current experimental results lead to the maximum value of the mixing parameter ϵ of the order 10^{-2} [27]. This mixing has been extensively studied in the literature (see Refs. [27–29] and references therein). The B − L gauged $U(1)'$ hidden sector scenario will also have a gauge coupling $g_{\rm B-L}$ as a free parameter in addition to its mass $m_{A'}$ and ϵ.

As mentioned in the previous section, even though one can consider all three parameters $(M_{A'}, \epsilon, g_{\rm B-L})$ to do a fit to the data, in the present work, we will focus on a model with only two free parameters, $M_{A'}$ and $g_{\rm B-L}$, and ignore the effect of kinetic mixing. Such analysis has not been done for experiments like TEXONO, LSND, or CHARM II. For BOREXINO and GEMMA, there is a study [30] which does not consider the interference effects. There are other studies using broken [31] and unbroken [32] $U(1)_{\rm B-L}$ scenarios to discuss neutrino-electron scattering.

Let us mention what is new in this study. First of all, the importance of interference effects which is overlooked in the literature is discussed. Our results show that interference effects are not always negligible and can enhance the results by as much as one order for some cases. Second, we obtain bounds on $g_{\rm B-L}$ without relating it through the bound on the kinetic mixing parameter ϵ. For this purpose the ϵ parameter is not considered at all. Third, the analyses for the TEXONO, LSND, and CHARM II data have been done for the first time, and we repeat analyses for GEMMA and BOREXINO and find out that, unlike the GEMMA case, the bound on $g_{\rm B-L}$ gets better for the BOREXINO data when the interference effects are included.

After these preliminary remarks, let us calculate the contributions of light dark photons to the neutrino-electron

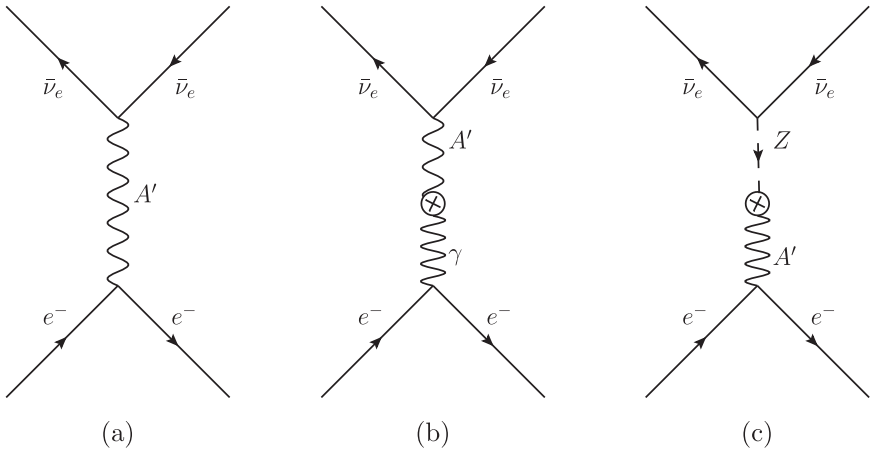

FIG. 2. Panel (a) shows the interactions of neutrinos with electrons via t-channel dark photon A' exchange. Panels (b) and (c) display for the kinetic mixing for photon–dark-photon and Z-boson–dark-photon interactions, respectively.

scattering processes (see Fig. 2). Note that the diagrams in Figs. 2(b) and 2(c) would exist only when there is a kinetic mixing between the dark photon and the SM neutral gauge bosons. Thus, such contributions are ignored.

The pure contribution of this new diagram to the neutrino-electron scattering is calculated, and the differential cross section is obtained as

$$\left[\frac{d\sigma}{dT}(\nu e^- \to \nu e^-)\right]_{\rm DP} = \frac{g^4_{\rm B-L} m_e}{4\pi E_\nu^2 (M^2_{A'} + 2m_e T)^2}(2E_\nu^2 + T^2 - 2TE_\nu - m_e T), \tag{5}$$

where the cross section is neutrino flavor blind.[1] For concreteness, it is assumed that A' has pure vector couplings of the form $\bar{f}\gamma^\mu f A'_\mu$. For deriving the cross section formula, neutrinos are assumed to be massless. One of the key points in this study is to calculate and discuss the effect of interference. Our analysis has shown that the contribution to cross sections from the interference of this gauged B − L model with the SM cannot be neglected for most of the neutrino-electron scattering experiments [30]. We discuss the criteria when the interference effects become sizable.

By using the diagrams given in Figs. 1 and 2(a), the interference differential cross section for each neutrino channel is obtained as

$$\frac{d\sigma_{\rm INT}(\nu_e e^-)}{dT} = \frac{g^2_{\rm B-L} G_F m_e}{2\sqrt{2} E_\nu^2 \pi (M^2_{A'} + 2mT)}(2E_\nu^2 - m_e T + \beta), \tag{6}$$

$$\frac{d\sigma_{\rm INT}(\bar{\nu}_e e^-)}{dT} = \frac{g^2_{\rm B-L} G_F m_e}{2\sqrt{2} E_\nu^2 \pi (M^2_{A'} + 2mT)}(2E_\nu^2 + 2T^2 - T(4E_\nu + m_e) + \beta), \tag{7}$$

$$\frac{d\sigma_{\rm INT}(\nu_\alpha e^-)}{dT} = \frac{g^2_{\rm B-L} G_F m_e}{2\sqrt{2} E_\nu^2 \pi (M^2_{A'} + 2mT)}(-2E_\nu^2 + m_e T + \beta), \tag{8}$$

$$\frac{d\sigma_{\rm INT}(\bar{\nu}_\alpha e^-)}{dT} = \frac{g^2_{\rm B-L} G_F m_e}{2\sqrt{2} E_\nu^2 \pi (M^2_{A'} + 2mT)}(-2E_\nu^2 - 2T^2 + T(4E_\nu + m_e) + \beta), \tag{9}$$

where the parameter β is defined as

$$\beta = \sin^2\theta_{\rm W}(8E_\nu^2 - 8E_\nu T - 4m_e T + 4T^2).$$

The index α in ν_α is either μ or τ, and they are different from the electron neutrino case, since only the Z-boson exchange diagram contributes in the former case, while both the Z- and W-boson exchange diagrams contribute in the latter. A detailed analysis of the interference effects will be given in the next section.

[1]The analytical expressions for the differential cross section in the SM, and pure DP cases, as well as that including the interference, are manually calculated and double-checked with the package program CalcHEP [33].

TABLE II. The key parameters of the TEXONO, LSND, CHARM II, BOREXINO and GEMMA measurements on $\nu - e$ scattering.

Experiment	Type of neutrino	$\langle E_\nu \rangle$	T	Measured $\sin^2\theta_W$
TEXONO-NPCGe [15]	$\bar{\nu}_e$	1–2 MeV	0.35–12 keV	⋯
TEXONO-HPGe [14]	$\bar{\nu}_e$	1–2 MeV	12–60 keV	⋯
TEXONO-CsI(Tl) [13]	$\bar{\nu}_e$	1–2 MeV	3–8 MeV	0.251 ± 0.039
LSND [18]	ν_e	36 MeV	18–50 MeV	0.248 ± 0.051
BOREXINO [16]	ν_e	862 keV	270–665 keV	⋯
GEMMA [17]	$\bar{\nu}_e$	1–2 MeV	3–25 keV	⋯
CHARM II [19]	ν_μ	23.7 GeV	3–24 GeV	0.2324 ± 0.0083
	$\bar{\nu}_\mu$	19.1 GeV	3–24 GeV	

IV. EXPERIMENTAL CONSTRAINTS

A. Neutrino-Electron scattering experiments

Neutrino scattering experiments are a good place to search for light dark photons. As seen from Eq. (5), for the low-mass region of $M_{A'}$ and for lower recoil energies of the electron, the differential cross section increases, which motivates us to search for new physics under such circumstances. Thus, experiments looking for dark matter particles or the neutrino magnetic moment, which requires low recoil energies, are good places to search these effects. Among them, for example, the TEXONO Collaboration in Taiwan has various sets of experiments, each of which is designed for different physics purposes with different recoil energy coverage.

These recoil ranges, as well as the average incident neutrino energies and the corresponding measured $\sin^2\theta_W$ values, are summarized in Table II. The table also includes the information for similar experiments like LSND, BOREXINO, GEMMA, and CHARM II. Since, for the larger mass values of $M_{A'}$, experiments with higher recoil energies of the electron with an energetic neutrino source will also be effected. This motivates us to search for the dark photon effects in the neutrino sector by using the LSND and CHARM II experiments, which measure $\sin^2\theta_W$ with the processes of ν_e and $\nu_\mu(\bar{\nu}_\mu)$ scattering, respectively.

A brief summary of the experiments listed in Table II would be useful here. The first in the list is the TEXONO experiment. The TEXONO Collaboration has a research program on low-energy neutrinos conducted at Kuo-Sheng Neutrino Laboratory, which is located at a distance of 28 m from one of the cores of the Kuo-Sheng Nuclear power station in Taiwan. Note that TEXONO is a reactor neutrino experiment with the advantage of high neutrino flux, hence the mean energy of neutrinos is $\langle E_\nu \rangle = 1$–2 MeV with a flux 6.4×10^{12} cm^{-2} s^{-1}.

Three different data sets of TEXONO, each of which are used for different purposes, have been analyzed. Let us summarize them below:

(1) **CsI:** A total mass of 187 kg CsI(Tl) crystal array is used to measure the $\bar{\nu}_e - e^-$ cross section with 29882/7369 kg-day of reactor ON/OFF data. The analysis range for the recoil energy of electrons is 3–8 MeV, and the Weinberg angle is measured with the data (see Table II).

(2) **HPGe:** Limits are set to the neutrino magnetic moment with a target mass of 1.06 kg HpGe detector. 570.7/127.8 kg-day of reactor ON/OFF exposure is taken, and a 10 keV analysis threshold with $\sim$1 kg^{-1} keV^{-1} day^{-1} background is achieved.

(3) **NPCGe:** N-type point-contact germanium detector of 500 g fiducial mass with 124.2 days reactor ON and 70.3 days reactor OFF data. A 0.3 keV threshold is achieved, used in a previous search of neutrino millicharge [15].

Unlike TEXONO, LSND (Liquid Scintillator Neutrino Detector) is a $\nu_e - e^-$ scattering experiment in which accelerator neutrinos are used as a source. Electron-neutrino beams are produced by the decaying of μ^+ at rest at the Los Alamos Neutron Science Center with a mean energy $\langle E_\nu \rangle \simeq 36$ MeV and total flux 11.76×10^{13} cm^{-2}. The analysis range for the recoil energy is $T \simeq 18$–50 MeV. The measured Weinberg angle is depicted in Table II by using a sample of 191 ± 22 events.

The CHARM II Collaboration measured electroweak parameters (see Table II) using ν_μ and $\bar{\nu}_\mu$ electron scattering based on 2677 ± 82 and 2752 ± 88 events, respectively. Neutrino beams are acquired via the decay of pions at CERN. The mean energy of $\langle E_{\nu_\mu} \rangle = 23.7$ GeV and $\langle E_{\bar{\nu}_\mu} \rangle = 19.1$ GeV. The energy range of the analysis is 3–24 GeV.

The BOREXINO Collaboration measured the spectrum of the ^{7}Be solar neutrino (with 862 keV energy) via the elastic scattering of neutrinos using a liquid scintillator. The analysis range for the recoil energy of electrons is 270–665 keV.

The GEMMA Collaboration measures the $\bar{\nu}_e - e$ scattering cross section, which can be used to put a bound on neutrino magnetic moments. Three years of data and a 1.5 kg HPGe detector with an energy threshold of 3 keV have been used. The average energy of the neutrino is $\langle E_\nu \rangle \sim 1$–2 MeV, and the $\bar{\nu}_e$ flux is 2.7×10^{13} cm^{-2} s^{-1}. For the analysis, 13000 ON-hours and 3000 OFF-hours of data are used.

Having shortly mentioned the experiments, let us summarize the procedure used in the analysis. The contribution of the dark photon to the electron recoil spectra is calculated as

$$\frac{dR_{\rm DP}}{dT} = t\rho_e \int_{E_{\nu_{\rm min}}} \frac{d\sigma_{\rm DP}}{dT}\frac{d\Phi(\bar{\nu}_e)}{dE_\nu} dE_\nu, \tag{10}$$

where ρ_e is the electron number density per kg of the target mass, t is the data-taking period, and $d\Phi/dE_\nu$ corresponds to the neutrino spectrum. For various $M_{A'}$ values, a minimum χ^2 fit is applied to find the 90% C.L. limits for the coupling constant $g_{\rm B-L}$ by defining it in the following form:

$$\chi^2 = \sum_{i=1} \left[\frac{R_{\rm Exp}(i) - (R_{\rm SM}(i) + R_{\rm DP}(i))}{\Delta_{\rm Stat}(i)}\right]^2,$$

where $R_{\rm SM}(i)$ and $R_{\rm DP}(i)$ are the expected event rate on the ith data bin due to SM and DP contributions, respectively, and $\Delta_{\rm Stat}(i)$ is the corresponding uncertainty in the measurement.

Let us analyze how the differential cross section at a fixed value of $g_{\rm B-L}$ changes as a function of T for various $M_{A'}$ values in Fig. 3. The chosen value for $g_{\rm B-L}$ is just representative. For larger $M_{A'}$ values like 0.1 MeV, 10 MeV, or 100 MeV, only the larger T tail of the differential cross section has some T dependency, but it becomes flat when T gets smaller than $M_{A'}$. This is expected, since as T gets much smaller than $M_{A'}$, the factor $(M_{A'}^2 + 2mT)^{-2} \to 1/M_{A'}^4$, and in addition to this, the other factor in the cross-section expression is dominated by E_ν in the small-T region. Overall, a flat profile is obtained. The point where the curves start being flat moves to smaller recoil energy T values as smaller and smaller $M_{A'}$ values are taken. The high sensitivity of the differential cross section to $M_{A'}$, which in turn gives better bounds of $g_{\rm B-L}$, is another motivation for searching for very light dark photons through $\nu - e$ scattering experiments.

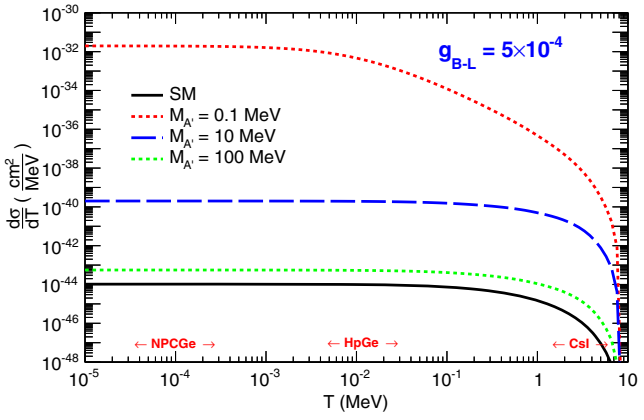

FIG. 3 (color online). Cross section versus recoil for various $M_{A'}$ by normalizing the neutrino flux to 1.

B. Roles of interference

A theme of this study is to explore the roles of interference effects between contributions from new physics and SM. The interference between the SM and new physics contributions due to vector boson exchange in neutrino-electron scattering processes is illustrated in Figs. 4(a) and 4(b), showing the exclusion limits for $g_{\rm B-L}$ versus $M_{A'}$ in TEXONO experiments [$\bar{\nu}_e$ at O(1 MeV)], together with LSND [ν_μ at O(10 MeV)] and CHARM II [ν_μ and $\bar{\nu}_\mu$ O(10 GeV)] experiments.

It can be seen from Fig. 4 that although for low recoil energies ($T \sim$ keV) the interference term does not affect the bound on the coupling constant $g_{\rm B-L}$, there is an enhancement in general due to interference for higher recoil energy values ($T \sim$ MeV). Contributions of interference terms are sizable when the effects due to new physics are small relative to the SM contributions. This is the case applicable to experiments where the SM cross-sections are measured, such as LSND, TEXONO-CsI, CHARM II, and BOREXINO, where the interference effects on the parameters $g_{\rm B-L}$ and $M_{A'}$ are depicted in Fig. 4. Otherwise, when the ranges of new physics effects are large compared to SM, the interference term can in general be neglected.

The interference effects between SM and new physics due to dark photons can be either constructive or destructive. As seen from Fig. 4, the interference is destructive only in the ν_μ electron scattering case of the CHARM II experiment. In all other cases, the interference is constructive, so that more stringent bounds can be derived. The behavior of the CHARM II result can be seen from Eq. (9), where the differential cross sections take the following forms:

$$\frac{d\sigma_{\rm INT}(\nu_\alpha e^-)}{dT} \propto T(T - 2E_\nu), \tag{11}$$

$$\frac{d\sigma_{\rm INT}(\bar{\nu}_\alpha e^-)}{dT} \propto -T(T - 2E_\nu), \tag{12}$$

with $\sin^2\theta_{\rm W} \simeq 1/4$. In general, $T/2 < E_{\nu_{\rm min}}$, such that the interference terms are always positive (constructive) or negative (destructive) for $\bar{\nu}_\alpha$ (ν_α), respectively. A similar analysis can be done for the ν_e and $\bar{\nu}_e$ scatterings, where the interference is constructive.

C. Results

With interference effects properly accounted for, the exclusion limits in the $M_{A'} - g_{\rm B-L}$ plane including all relevant neutrino-electron scattering experiments are shown in Fig. 5. The BOREXINO results [30] with interference are included, provided better bounds by about 30%. It was verified that switching off the interference term would

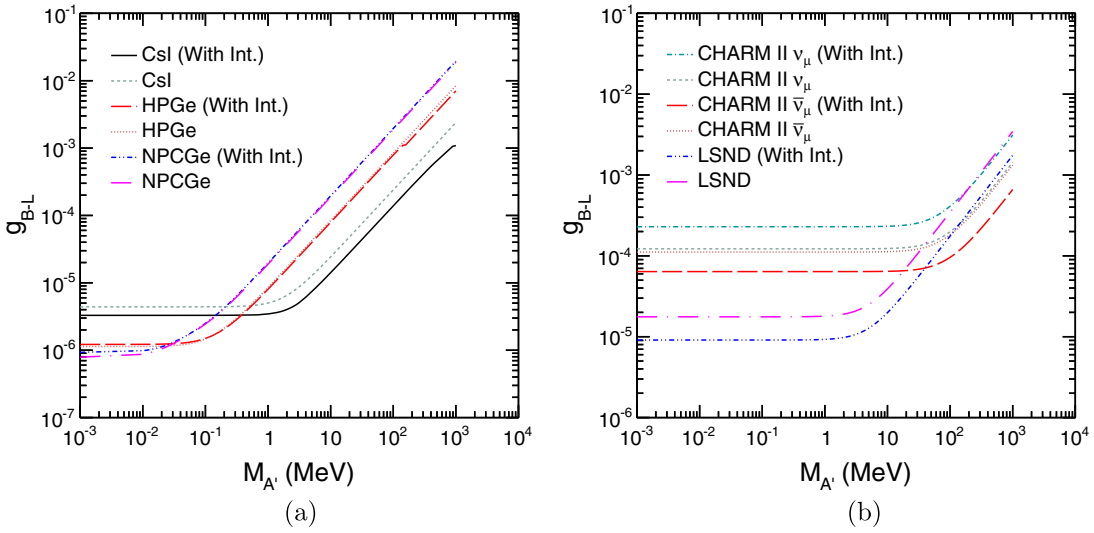

FIG. 4 (color online). The 90% C.L. exclusion limits in the $g_{\mathrm{B-L}} - M_{A'}$ plane for various TEXONO experiments in panel (a), and for the LSND and CHARM II experiments in panel (b). The results with and without the interference contributions are shown to highlight its significance.

reproduce the results of Ref. [30]. The best limits for different parts of exclusion regions come from different reactor neutrino experiments: by GEMMA and TEXONO-CsI for $M_{A'} < 0.1$ MeV and $0.1 < M_{A'} < 100$ MeV, respectively, and by accelerator neutrino data from CHARM II ($\bar{\nu}_\mu$) for $M_{A'} > 100$ MeV. We adopted the analysis of Ref. [30] to derive bounds on $(M_{A'} - g_{\mathrm{B-L}})$ from anomalous dark photon contributions to $\bar{\nu}_e - e^-$ scattering data in GEMMA. Our results indicate that at low recoil energies, the interference effects between the SM and DP contributions are small.

The behavior of the exclusion curves of Fig. 5 can be understood through the dark photon cross section

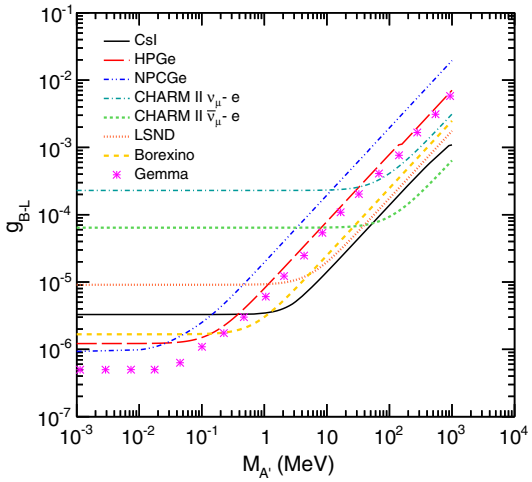

FIG. 5 (color online). The 90% C.L. exclusion limits of the gauge coupling constant $g_{\mathrm{B-L}}$ of the $U(1)_{\mathrm{B-L}}$ group as a function of the dark photon mass $M_{A'}$ by including interference effects. The regions above the curves are excluded.

expression of Eq. (5), with a dependence of $(M_{A'}^2 + 2mT)^{-2}$. Accordingly, studies of dark photons favor experiments with low-energy neutrinos like those from reactors. At $M_{A'} \ll T$, the cross section is insensitive to $M_{A'}$, implying that (i) neutrino-electron scattering experiments would not be able to resolve dark photons with mass less than keV, which is the lower reach of current sensitivities on T; (ii) accelerator experiments with E_ν and T at the GeV range would not provide good sensitivities, except at $M_{A'}$ also larger than GeV.

Exclusion regions from the $\nu - e$ scattering experiments are displayed with other laboratory and cosmological bounds in Fig. 6, which corresponds to an update of Fig. 8(a) in Ref. [30] with recent data. The dark color shadings correspond to limits from laboratory experiments where data were taken under controlled conditions and interpretations are model independent. Constraints in light shadings typically involve astrophysical modeling as well as implicit assumptions and choice of parameters.

A few comments on the recent data in Fig. 6 are in order. The data of the other laboratory and cosmological bounds which are plotted on the kinetic mixing ϵ and $M_{A'}$ plane can be used to constrain $g_{\mathrm{B-L}}$. The conversion is $\epsilon \to \frac{(\mathrm{B-L})(f)}{Q_f} g_{\mathrm{B-L}}$ for experiments not involving decay modes of the dark photon. Otherwise, the conversion would have the additional factor $\left(\frac{\mathrm{BR}(A' \overset{B-L}{\to} f\bar{f})}{\mathrm{BR}(A' \overset{\epsilon}{\to} f\bar{f})}\right)^{1/2}$ on the right-hand side for experiments involving A' decaying to fermions.

The excluded regions labeled as "Sun" and "Globular Clusters" are originally presented in Refs. [48,49]. Recently, it has been shown in Ref. [50] that emission of the forgotten longitudinal modes of the dark photon change the stellar constraints drastically, especially in the

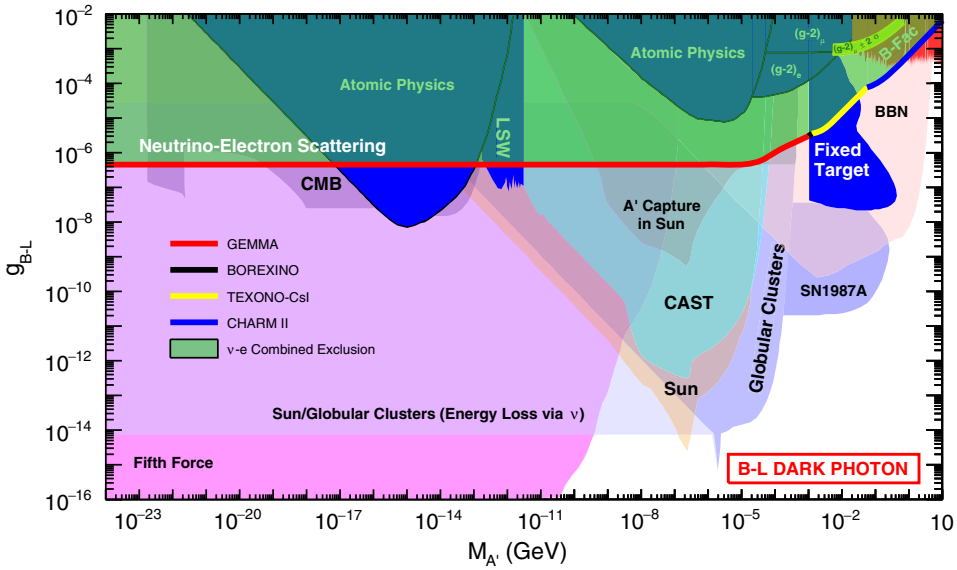

FIG. 6 (color online). The current global exclusion plot of the bounds on the gauge coupling of the dark photon from different cosmological and astrophysical sources as well as laboratory experiments, adapted from Ref. [30] with combined limits from neutrino-electron scattering (this work) overlaid. The 90% C.L. bounds are defined by the GEMMA, BOREXINO, TEXONO-CsI, and CHARM II ($\bar{\nu}_\mu$) experiments, from low to high $M_{A'}$. Data from $\nu - e$ scattering significantly improve the bounds among controlled laboratory experiments in much of the $M_{A'}$ range. The principles of the different categories of experiments are summarized in Table III.

small-$M_{A'}$ region. Consequently, the region excluded by the so-called light-shining-through-wall (LSW) experiments falls under the tails of the excluded regions from the stellar bounds [50].

The constraints of big bang nucleosynthesis (BBN) on the mass of a light vector boson and its coupling constant to neutrinos was first studied in Ref. [55]. Subsequent detailed analysis [32] for the B − L scenario with light right-handed Dirac neutrinos opens the possibility for them to be thermalized through dark photon exchange, which would contribute to the extra number of neutrino species $\Delta N_{\rm eff}$. The BBN bounds of $\Delta N_{\rm eff} < 1$ at 95% C.L. with the use of ^{4}He abundance data [54] can be translated to the constraints on $g_{\rm B-L}$ and $M_{A'}$ [32] depicted in Fig. 6. In the case of Dirac neutrinos, the BBN gives a better bound than the ones from the neutrino-electron scattering experiments in much of the $M_{A'}$ region.

Exclusions from the recent *BABAR* data [40], marked "B-Fac" in Fig. 6, cover a wider $M_{A'}$ region. The 2σ allowed band from the muon $g-2$ experiment [3] is also shown. Part of the allowed band ($M_{A'} \gtrsim 0.02$ GeV) is rejected by "B-Fac" data (see also the proposal [56] to probe the lower $M_{A'}$ regions). Results from neutrino-electron scattering experiments also probe and exclude

TABLE III. The list of different sources used to bound the gauge coupling of the dark photon. The details of each are summarized very briefly together with references for the details.

Experiments	Comments	References
$g-2$	A' contribution to magnetic moment of e and μ.	[3,34]
Fixed Target	A' production in beam dump experiments. $A' \to e^- e^+$ in $M_{A'} > 2m_e$.	[28,35–39]
B factories	$\Upsilon \to \gamma A'$ and $A' \to \gamma l^+ l^-$. Sensitive to range 0.02 GeV $< M_{A'} <$ 10.2 GeV.	[29,40–42]
Fifth force	Precision measurements of gravitational, Casimir and Van der Waals forces. Sensitive to $M_{A'} \lesssim 100$ eV.	[43,44]
Atomic Physics	Corrections to Coulomb force.	[43,45]
Supernova	Analysis of energy loss of supernova.	[46,47]
Sun	Luminosity analysis in the conversion of plasmons in the Sun.	[48–50]
LSW	Transition of laser $\to A' \to \gamma$.	[43,51]
CMB	Study of black-body spectrum of Cosmic Microwave Background.	[43,52]
CAST	Comparison of flux of dark and usual photon.	[48,53]
Globular clusters	Energy loss due to dark photons in globular clusters.	[43,48–50]
BBN	Thermalization of Dirac neutrinos ν_R via A', contributing to the effective new neutrino species $\Delta N_{\rm eff}$.	[32,54]

that region by an order of magnitude. There is another scenario discussed in Ref. [57] in which a gauged $U(1)_L$ is proposed as an alternative to $U(1)_{\mathrm{B-L}}$. As far as the $g-2$ of the muon favored region is concerned, it does better in $U(1)_L$ than the one in $U(1)_{\mathrm{B-L}}$ against certain constraints to which the B − L gauge boson is sensitive. However, the scenario falls short against the neutrino-electron scattering bounds from BOREXINO solar neutrino flux measurements.

It can be seen from Figs. 5 and 6 that the bounds on $g_{\mathrm{B-L}}$ from $\nu-e$ scattering experiments are insensitive to $M_{A'}$ at $M_{A'} < 10$ keV. The constraints are not expected to change drastically, since it is experimentally challenging to measure even lower recoil energies. The $\nu-e$ scattering data significantly improve the bounds among the controlled laboratory experiments over much of the parameter space. The sharp cutoff at $2m_e$ for "Fixed Target" experiments is based on the channel $A' \to e^+e^-$. The gap at $M_{A'} \simeq 10^{-3}$ GeV is expected to be probed when invisible channels like $A' \to 2\nu$ in the case of B − L dark photons would be taken into account.

V. CONCLUSIONS

A very light dark photon from the hidden sector through a vector portal could couple to some SM particles, which might give a signal via neutrino-electron scattering experiments if, especially, the dark photon is the gauge field of a $U(1)$ group gauged with B − L symmetry. Indeed, this will allow a direct coupling with neutrinos, which modifies the electroweak contribution with a presumed negligible interference. The new interactions due to the existence of A' bosons whose couplings do not contain derivatives lead to the differential cross section being proportional to $1/T^2$, which makes low-energy neutrino experiments sensitive to dark photon searches in the low-mass region. Hence, low-energy neutrino experiments like TEXONO, which aims to measure neutrino nucleus coherent scattering as well as the neutrino magnetic moment, has an advantage in searching for new gauged bosons located much below the electroweak scale. For the higher-mass region for A' bosons, neutrino experiments with higher incident energy have better sensitivity.

We have done a study to search for the signal of dark photons originating from a $U(1)_{\mathrm{B-L}}$ group in the available data sets of the TEXONO as well as GEMMA, BOREXINO, LSND, and CHARM II. With no signal, our analysis is converted to a bound on the gauge coupling $g_{\mathrm{B-L}}$ as a function of $M_{A'}$. A crucial aspect of our study is in the interference effects between the dark photon and SM contributions in neutrino-electron scattering. Our results show that the interference effects are significant for experiments with a smaller deviation from the SM prediction. Other than the CHARM II ν_μ electron scattering case, all the others have constructive interference which makes the bounds more stringent. The BOREXINO case, where the interference effects are sizable, is updated. Our results with neutrino-electron scattering expand the excluded regions among the controlled laboratory measurements. The experimental bounds would not be improved significantly by the future neutrino experiments, since the pure new physics differential cross section is proportional to the fourth power of the coupling constant $g^4_{\mathrm{B-L}}$.

ACKNOWLEDGMENTS

I. T. and S. B. thank METU-BAP Grant No. 08-11-2013-028. I. T. also thanks TUBA-GEBIP for its partial support. S. B. acknowledges the TUBITAK-2211 program for its partial support. T. M. A. thanks the Visiting Professor program at King Saud University for its partial support. H. T. W. and L. S. are supported by the ECP Program from the National Center of Theoretical Science in Taiwan. We thank R. Harnik for sending us the pdf version of Fig. 8(a) in Ref. [30]. We are grateful to G. Krnjaic for useful correspondences and B. Echenard for providing us the recent *BABAR* data. I. T. and S. B are thankful to Altug Ozpineci for bringing the LATEX TikZ package to their attention.

We thank R. Harnik for bringing Ref. [50] to our attention.

[1] H. T. Wong, H. B. Li, J. Li, Q. Yue, and Z. Y. Zhou, Research program towards observation of neutrino-nucleus coherent scattering, J. Phys. Conf. Ser. **39**, 266 (2006); Conf. Proc. C **060726**, 344 (2006).

[2] J. Beringer *et al.* (Particle Data Group), Review of particle physics, Phys. Rev. D **86**, 010001 (2012), and 2013 update for the 2014 edition (URL: http://pdg.lbl.gov).

[3] G. W. Bennett *et al.* (Muon G-2 Collaboration), Final report of the muon E821 anomalous magnetic moment measurement at BNL, Phys. Rev. D **73**, 072003 (2006).

[4] C. A. Baker, D. D. Doyle, P. Geltenbort, K. Green, M. G. D. van der Grinten, P. G. Harris, P. Iaydjiev, S. N. Ivanov *et al.*, An Improved Experimental Limit on the Electric Dipole Moment of the Neutron, Phys. Rev. Lett. **97**, 131801 (2006).

[5] R. Pohl, A. Antognini, F. Nez, F. D. Amaro, F. Biraben, J. M. R. Cardoso, D. S. Covita, A. Dax *et al.*, The size of the proton, Nature (London) **466**, 213 (2010).

[6] J. Chang, J. H. Adams, H. S. Ahn, G. L. Bashindzhagyan, M. Christl, O. Ganel, T. G. Guzik, J. Isbert *et al.*, An excess of cosmic ray electrons at energies of 300–800 GeV, Nature (London) **456**, 362 (2008).

[7] O. Adriani *et al.* (PAMELA Collaboration), An anomalous positron abundance in cosmic rays with energies 1.5–100 GeV, Nature (London) **458**, 607 (2009).

[8] M. Ackermann *et al.* (Fermi LAT Collaboration), Measurement of Separate Cosmic-ray Electron and Positron Spectra with the Fermi Large Area Telescope, Phys. Rev. Lett. **108**, 011103 (2012).

[9] P. Jean, J. Knoedlseder, V. Lonjou, M. Allain, J.-P. Roques, G. K. Skinner, B. J. Teegarden, G. Vedrenne *et al.*, Early SPI/INTEGRAL measurements of 511 keV line emission from the 4th quadrant of the Galaxy, Astron. Astrophys. **407**, L55 (2003).

[10] R. Bernabei *et al.* (DAMA Collaboration), First results from DAMA/LIBRA and the combined results with DAMA/NaI, Eur. Phys. J. C **56**, 333 (2008).

[11] P. Sreekumar *et al.* (EGRET Collaboration), EGRET observations of the extragalactic gamma-ray emission, Astrophys. J. **494**, 523 (1998).

[12] M. Aguilar *et al.* (AMS Collaboration), First Result from the Alpha Magnetic Spectrometer on the International Space Station: Precision Measurement of the Positron Fraction in Primary Cosmic Rays of 0.5350 GeV, Phys. Rev. Lett. **110**, 141102 (2013).

[13] M. Deniz *et al.*, Measurement of $\bar{\nu}_e$-electron scattering cross-section with a CsI(Tl) scintillating crystal array at the Kuo-Sheng nuclear power reactor, Phys. Rev. D **81**, 072001 (2010).

[14] H. B. Li *et al.*, Limit on the Electron Neutrino Magnetic Moment from the Kuo-Sheng Reactor Neutrino Experiment, Phys. Rev. Lett. **90**, 131802 (2003); A search of neutrino magnetic moments with a high-purity germanium detector at the Kuo-Sheng nuclear power station, Phys. Rev. D **75**, 012001 (2007).

[15] J. W. Chen, H. C. Chi, H. B. Li, C.-P. Liu, L. Singh, H. T. Wong, C. L. Wu, and C. P. Wu, Constraints on millicharged neutrinos via analysis of data from atomic ionizations with germanium detectors at sub-keV sensitivities, Phys. Rev. D **90**, 011301 (2014).

[16] G. Bellini, J. Benziger, D. Bick, S. Bonetti, G. Bonfini, M. Buizza Avanzini, B. Caccianiga, L. Cadonati *et al.*, Precision Measurement of the ^{7}Be Solar Neutrino Interaction Rate in Borexino, Phys. Rev. Lett. **107**, 141302 (2011).

[17] A. G. Beda, E. V. Demidova, A. S. Starostin, V. B. Brudanin, V. G. Egorov, D. V. Medvedev, M. V. Shirchenko, and T. Vylov, GEMMA experiment: Three years of the search for the neutrino magnetic moment, Phys. Part. Nucl. Lett. **7**, 406 (2010).

[18] L. B. Auerbach *et al.*, Measurement of electron-neutrino electron elastic scattering, Phys. Rev. D **63**, 112001 (2001).

[19] P. Vilain *et al.*, Measurement of dierential cross-sections for muon-neutrino electron scattering, Phys. Lett. B **302**, 351 (1993); , Precision measurement of electroweak parameters from the scattering of muon-neutrinos on electrons, Phys. Lett. B **335**, 246 (1994).

[20] E. Bulbul, M. Markevitch, A. Foster, R. K. Smith, M. Loewenstein, and S. W. Randall, Detection of an unidentied emission line in the stacked X-ray spectrum of Galaxy clusters, Astrophys. J. **789**, 13 (2014).

[21] L. B. Okun, Zh. Eksp. Teor. Fiz. **83**, 892 (1982) [Limits of electrodynamics: paraphotons?, Sov. Phys. JETP **56**, 502 (1982)].

[22] B. Holdom, Two U(1)'s and epsilon charge shifts, Phys. Lett. B **166**, 196 (1986).

[23] B. Kayser and R. E. Shrock, Distinguishing between Dirac and Majorana neutrinos in neutral current reactions, Phys. Lett. B **112**, 137 (1982).

[24] J. Barranco, D. Delepine, V. G. Macias, C. Lujan-Peschard, and M. Napsuciale, Scattering processes could distinguish Majorana from Dirac neutrinos, Phys. Lett. B **739**, 343 (2014).

[25] M. Deniz *et al.* (TEXONO Collaboration), Constraints on non-standard neutrino interactions and unparticle physics with neutrino-electron scattering at the Kuo-Sheng nuclear power reactor, Phys. Rev. D **82**, 033004 (2010).

[26] S. Bilmis, M. Deniz, H. B. Li, J. Li, H. Y. Liao, S. T. Lin, V. Singh, H. T. Wong *et al.*, Constraints on non-commutative physics scale with neutrino-electron scattering, Phys. Rev. D **85**, 073011 (2012).

[27] R. Essig, J. A. Jaros, W. Wester, P. H. Adrian, S. Andreas, T. Averett, O. Baker, B. Batell *et al.*, Working group report: new light weakly coupled particles, arXiv:1311.0029.

[28] R. Essig, R. Harnik, J. Kaplan, and N. Toro, Discovering new light states at neutrino experiments, Phys. Rev. D **82**, 113008 (2010).

[29] R. Essig, P. Schuster, and N. Toro, Probing dark forces and light hidden sectors at low-energy e^+e^- colliders, Phys. Rev. D **80**, 015003 (2009).

[30] R. Harnik, J. Kopp, and P. A. N. Machado, Exploring ν signals in dark matter detectors, J. Cosmol. Astropart. Phys. 07 (2012) 026.

[31] M. Williams, C. P. Burgess, A. Maharana, and F. Quevedo, New constraints (and motivations) for abelian gauge bosons in the MeV-TeV mass range, J. High Energy Phys. 08 (2011) 106.

[32] J. Heeck, Unbroken B-L Symmetry, Phys. Lett. B **739**, 256 (2014).

[33] A. Belyaev, N. D. Christensen, and A. Pukhov, CalcHEP 3.4 for collider physics within and beyond the Standard Model, Comput. Phys. Commun. **184**, 1729 (2013).

[34] M. Pospelov, Secluded U(1) below the weak scale, Phys. Rev. D **80**, 095002 (2009).

[35] J. D. Bjorken, R. Essig, P. Schuster, and N. Toro, New fixed-target experiments to search for dark gauge forces, Phys. Rev. D **80**, 075018 (2009).

[36] B. Batell, M. Pospelov, and A. Ritz, Exploring portals to a hidden sector through fixed targets, Phys. Rev. D **80**, 095024 (2009).

[37] E. Izaguirre, G. Krnjaic, P. Schuster, and N. Toro, Physics motivation for a pilot dark matter search at Jeerson laboratory, Phys. Rev. D **90**, 014052 (2014).

[38] M. D. Diamond and P. Schuster, Searching for Light Dark Matter with the SLAC Millicharge Experiment, Phys. Rev. Lett. **111**, 221803 (2013).
[39] S. Abrahamyan *et al.* (APEX Collaboration), Search for a New Gauge Boson in Electron-Nucleus Fixed-Target Scattering by the APEX Experiment, Phys. Rev. Lett. **107**, 191804 (2011).
[40] J. P. Lees *et al.* (*BABAR* Collaboration), Search for a Dark Photon in e^+e^- Collisions at *BABAR*, Phys. Rev. Lett. **113**, 201801 (2014).
[41] C. D. Carone and H. Murayama, Possible Light U(1) Gauge Boson Coupled to Baryon Number, Phys. Rev. Lett. **74**, 3122 (1995).
[42] M. L. Graesser, I. M. Shoemaker, and L. Vecchi, A dark force for baryons, arXiv:1107.2666.
[43] J. Jaeckel and A. Ringwald, The low-energy frontier of particle physics, Annu. Rev. Nucl. Part. Sci. **60**, 405 (2010).
[44] E. G. Adelberger, B. R. Heckel, S. A. Hoedl, C. D. Hoyle, D. J. Kapner, and A. Upadhye, Particle Physics Implications of a Recent Test of the Gravitational Inverse Sqaure Law, Phys. Rev. Lett. **98**, 131104 (2007).
[45] D. F. Bartlett and S. Logl, Limits On An Electromagnetic Fifth Force, Phys. Rev. Lett. **61**, 2285 (1988).
[46] J. B. Dent, F. Ferrer, and L. M. Krauss, Constraints on light hidden sector gauge bosons from supernova cooling, arXiv:1201.2683.
[47] D. Kazanas, R. N. Mohapatra, S. Nussinov, V. L. Teplitz, and Y. Zhang, Supernova bounds on the dark photon using its electromagnetic decay, Nucl. Phys. B **890**, 17 (2015).
[48] J. Redondo, Helioscope bounds on hidden sector photons, J. Cosmol. Astropart. Phys. 07 (2008) 008.
[49] G. G. Raffelt and G. D. Starkman, Stellar energy transfer by keV mass scalars, Phys. Rev. D **40**, 942 (1989).
[50] H. An, M. Pospelov, and J. Pradler, New stellar constraints on dark photons, Phys. Lett. B **725**, 190 (2013).
[51] M. Ahlers, H. Gies, J. Jaeckel, J. Redondo, and A. Ringwald, Laser experiments explore the hidden sector, Phys. Rev. D **77**, 095001 (2008).
[52] A. Mirizzi, J. Redondo, and G. Sigl, Microwave background constraints on mixing of photons with hidden photons, J. Cosmol. Astropart. Phys. 03 (2009) 026.
[53] E. Arik *et al.* (CAST Collaboration), Probing eV-scale axions with CAST, J. Cosmol. Astropart. Phys. 02 (2009) 008.
[54] G. Mangano and P. D. Serpico, A robust upper limit on $N_{\rm eff}$ from BBN, circa 2011, Phys. Lett. B **701**, 296 (2011).
[55] B. Ahlgren, T. Ohlsson, and S. Zhou, Comment on Is Dark Matter with Long-Range Interactions a Solution to All Small-Scale Problems of Cold Dark Matter Cosmology?, Phys. Rev. Lett. **111**, 199001 (2013).
[56] Y. Kahn, G. Krnjaic, J. Thaler, and M. Toups, DAEALUS and dark matter detection, Phys. Rev. D **91**, 055006 (2015).
[57] H. S. Lee, Muon $g-2$ anomaly and dark leptonic gauge boson, Phys. Rev. D **90**, 091702 (2014).